JOURNAL OF APPLIED ELECTROCHEMISTRY 2 (1971) 23–29

An optical cell for photographic studies of gas evolution during molten salt electrolysis

P. L. KING* AND B. J. WELCH

School of Chemical Technology, The University of New South Wales, Kensington, N.S.W., Australia.

Received 2 July 1971

The simple optical cell described is useful for providing supplementary information on the evolution of gases during the electrolysis of fused salts or other electrolytes. Its use with PbS–$PbCl_2$ and PbS–$PbCl_2$–NaCl melts demonstrated that, for anodic sulphur gas production, residual gas evolution occurs, indicating the formation of a chemisorbed species as a reaction intermediate. Dissolution of the sulphur in the melt also takes place; its rate increases with increase in temperature and sulphide concentration.

1. Introduction

Recent publications [1–5] have shown the importance of making surface, optical, spectral, and kinetic studies of processes associated with electrode kinetics and gas evolution during the electrolysis.

In fused salts optical studies are hindered because of the surrounding heating system that is necessary to attain the high operating temperatures involved. However, it is particularly desirable to make studies in this class of system because of the important effect dissolution of gases has on Faradaic processes, since it is usually via a dissolution mechanism that recombination is facilitated [5–7]. The methods hitherto used for kinetic studies in fused salts [8, 9] have only been adequate for mechanistic interpretation of the combined effects of gas dissolution and subsequent reaction. They have been unable to simulate or discern processes occurring at or near the electrode surface, nor have they been able to provide instantaneous rate data for known operating conditions.

Although the technique described here was developed to establish conclusively the dissolution of sulphur in molten salt solutions containing lead sulphide, it was found to provide other valuable information on the electrode reaction mechanism. It is particularly suitable where the melts being studied are intensely coloured, and visual observations are not otherwise possible, as is the case in the example used. From the results obtained and other experiences in our department we consider this inexpensive method invaluable for several purposes. By co-ordinating the optical study with the appropriate electrochemical programme, the method is useful for detecting or confirming the following:

—the dissolution of the gas or gases evolved at the electrode;
—the rate of this dissolution as a function of operating conditions;
—the phenomenon of residual gas evolution, which is related to reaction mechanism [4, 10];
—the initiation period for the gas evolution;
—the change in electrode process and accompanying change in electrochemical products (e.g. from solid to gas).

The first four of these points are illustrated in this paper in support of the optical cell as a supplementary research tool.

* Present address: Central Laboratory, The Colonial Sugar Refining Company Ltd., Pyrmont, N.S.W., Australia.

The cell is similar to thin layer cells used for coulometric analytical purposes [11], but with the essential difference that the electrodes are positioned at right angles to those in the former case. Consequently, because of the thin cross-section, the gaseous product formed is trapped adjacent to the electrode surface but remote from the counter electrode. Because all gases evolved soon form cylindrical shapes, due to having growth restricted in one dimension, the volume of product formed during electrolysis can be readily assessed, provided the formula is known. Photographic recording permits a coulometric correlation and kinetic interpretation.

2. Construction of The Optical Cell

The cell assembly consisted of two polished glass microscope slides sandwiched together with the thin electrodes acting as spacers, as is shown in Fig. 1. The cell volume could be varied by changing the electrode thickness (within limitations imposed by the filling method), or the interelectrode separation, which could also be varied readily.

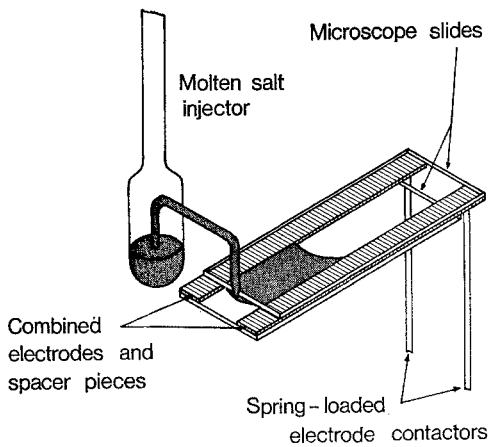

Fig. 1. Molten salt optical cell.

The cell assembly was held in a horizontal plane in the centre of the furnace in two slots in a (40 mm i.d. × 50 mm o.d.) aluminous tube (Fig. 2). This tube was supported by a brass endpiece which clamped to the lower end of the furnace tube. The endpiece supported, in PTFE bushes, the spring-loaded nickel rods which made contact with the cell electrodes, and the spring-loaded inverted stirrup which clamped the cell assembly firmly in place. A glass window mounted in silicone rubber gave an optical path up the centre of the alumina tube. The inert gas inlet was arranged just above the window to cool it and to sweep away vapours (e.g. $PbCl_2$) which might deposit on it.

The top of the furnace was closed with a polished Armourglass disc, and could be sealed with

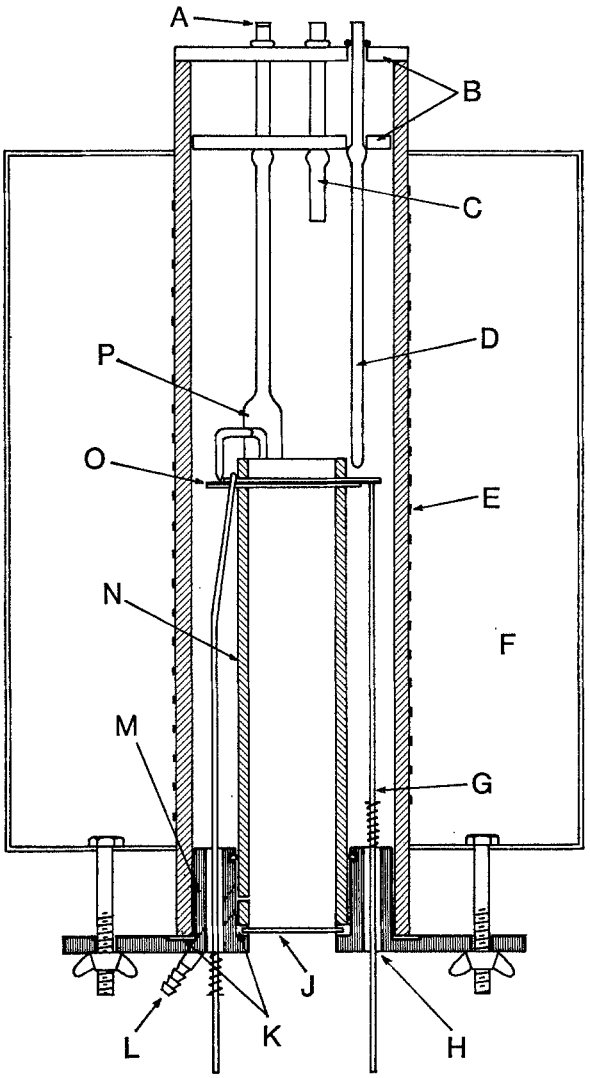

Fig. 2. Molten salt optical cell: furnace arrangement. A—silicone rubber septum; B—Armourglass; C—gas outlet; D—thermocouple well; E—Kanthal resistance wire furnace winding; F—kieselguhr furnace insulation; G—spring-loaded electrode contactor; H—PTFE bushes; J—window; K—silicone rubber seals; L—inert gas inlet; M—brass endpiece; N—alumina tube; O—optical cell; P—molten salt injector.

a silicone elastomer. A second glass disc suspended lower in the furnace served to position tubes and minimize convective heat losses. Holes through the discs permitted the insertion of a thermocouple well, a gas outlet, and the molten salt injector. These tubes were sealed into the holes with PTFE taped silicone O-rings.

The molten salt injector consisted of a reservoir containing the salt, with a delivery tube leading to the cell inlet. Application of a controlled gas pressure in the injector, by insertion of a syringe through the silicone rubber septum at the top of the injector, caused the molten salt to flow out of the delivery tube at the cell inlet. The molten salt surface-tension resulted in it being drawn into the cell by capillary action providing the electrode thickness was not too great.

The results of electrolysis between the two electrodes could be monitored visually and recorded photographically for subsequent examination and measurement. For this the cell was illuminated with a photoflood mounted above the furnace. In this study photographic recording could be made with either a 35 mm still camera, or a 16 mm movie camera with a long focus lens. The cameras were mounted below the furnace. It was found the movie camera could be better co-ordinated with the electrolysis system when this was desired for precise rate studies. However, the 35 mm camera was invaluable for exploratory studies, such as establishing the occurrence of dissolution of the electrochemically formed gas, or less precise kinetic studies.

The furnace used to heat the optical cell is also shown in Fig. 2. The kanthal heating element was wound on a 9 cm i.d. fused silica tube that was approximately 38 cm in total length. This could be heated and controlled using normal methods.

In the electrochemical cell described all conventional two-electrode voltammetric and coulometric studies could be made using the conventional equipment used in electrochemical studies. If a reference electrode is necessary, one of similar design to the molten salt injector can be used, but invariably IR compensation will be necessary.

The experimental results presented are from constant current electrolysis using strips of Union Carbide A.U.C. grade graphite as electrodes. The electrodes (approximately 70 mm long × 6 mm wide × 0·8 mm thick) had faces ground to a smooth and parallel finish prior to use. When the working area needs to be defined the face of the lead-in section can be insulated with, for example, a layer of boron nitride paint.

2.1 *Experimental Procedure*

Two different solvents were used for the PbS, these were $PbCl_2$ and the eutectic composition 73 mole% $PbCl_2$ + 27 mole% NaCl. A.R. grade chemicals were used and the chlorides were purified before the PbS was added. All samples were pre-fused then ground, and the injector filled with the powder. This ensured ready fusion to form a homogeneous solution in the injector.

Fig. 3 shows two typical frames from a photographic recording. These illustrate how the gas bubbles become entrapped in the cell during electrolysis (Fig. 3A) and their subsequent dissolution (Fig. 3B). It can be seen that the volume of the bubbles can be accurately estimated, as can the area of the gas–liquid interface, providing allowance is made for the meniscus shape. For dissolution studies several individual bubbles can be studied separately, thus providing a simultaneous cross-check on the reaction rate.

In calculating the theoretical volumes of the gaseous sulphur for comparison during electrolysis, allowance must be made for the various molecular forms that exist. The data of Braune *et al* [12] was used for this purpose.

3. Results

3.1 *Residual gas evolution*

Janssen and Hoogland [4, 10] have recently demonstrated that if an overall gas evolution reaction of the type

$$2\ X^{n-} \rightarrow X_2 + 2ne$$

proceeds by the following mechanism

$$X^{n-} \rightarrow X(\text{ads}) + ne \quad \text{(Fast)}$$
$$X^{n-} + X(\text{ads}) \rightarrow X_2 + ne \quad \text{(Rate determining)}$$

then residual gas evolution (R.G.E.) will occur on ceasing electrolysis. This gas evolution is due

to slow desorption of the adsorbed atomic species according to the equation

$$X(\text{ads}) + X(\text{ads}) \rightarrow X_2.$$

Thus detecting either the occurrence or absence of R.G.E. is an invaluable diagnostic tool in the evaluation of reaction mechanisms involving gases and can prevent erroneous interpretations [13].

In the application from this optical cell the volume of gas evolved is measured as a function of time, by the tedious process of summing the volume of all gas bubbles evolved during constant current electrolysis and also after ceasing the electrolysis. This method has an advantage over the elegant method of Janssen and Hoogland [4] by providing the volume–time relationship during the initial period of electrolysis. This provides a cross-check on the mechanism since, if R.G.E. is due to the type of mechanism described above, the initial rate of evolution will be low due to the build-up of the equilibrium concentration of absorbed species on the electrode surface. Such a check is particularly useful if dissolution of the gas occurs (as is the case in this system), since R.G.E. will only be directly measurable if the rate of R.G.E. is greater than the rate of dissolution.

The occurrence of R.G.E. is illustrated in Fig. 4 for two different electrolysis times. The experimental conditions for these curves (i.e. 445°C and 5% PbS) are such that the rate of dissolution of sulphur is very slow (see Fig. 6). Although these curves are for different electrolysis times they each show three characteristic regions which are:

(i) The build-up of the chemisorbed layer. This occurs over the first 30 seconds, during which only a small volume of gas is evolved.
(ii) Steady evolution of gaseous sulphur. This follows the build-up of the chemisorbed layer and occurs at approximately theoretical rate until cessation of electrolysis.
(iii) R.G.E. The amount of gas evolved is approximately the same in each case, and equal to the amount evolved during about 30 seconds of electrolysis when a steady rate of evolution is achieved.

At higher sulphide concentrations and higher temperatures the R.G.E. is not as easily detected due to the rapid dissolution of the sulphur. However, under these conditions the build-up of the chemisorbed layer is still evident as is

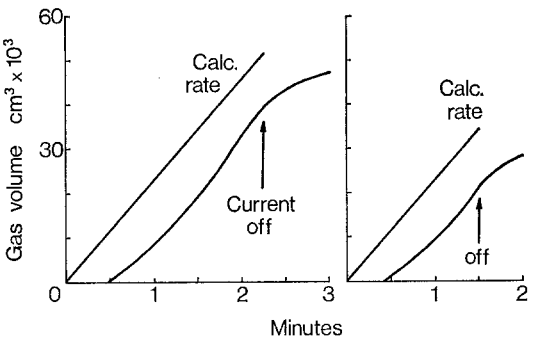

Fig. 4. Volume of sulphur evolved as a function of time, during and after constant current electrolysis at 10 mA. Electrolyte—5% PbS in $PbCl_2$-NaCl at 445°C.

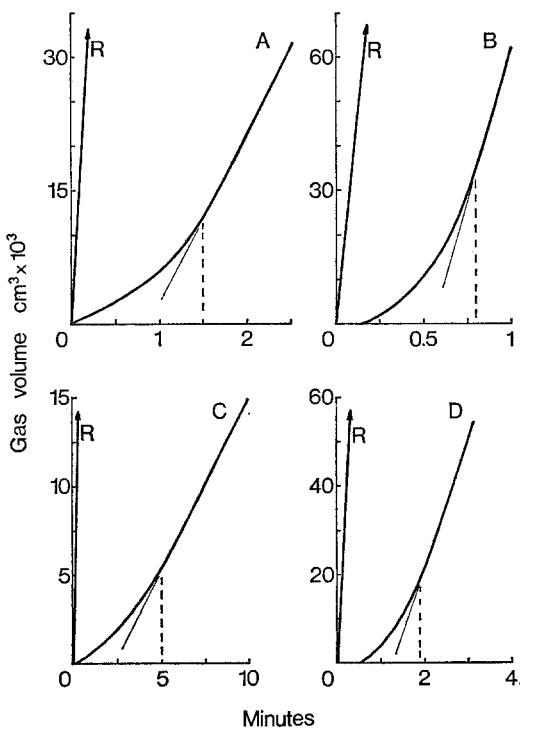

Fig. 5. Time required to establish a steady rate of gas evolution at 530°C.
A: 20% PbS in $PbCl_2$. i=50 mA.
B: 5% PbS in $PbCl_2$. i=100 mA.
C: 5% PbS in $PbCl_2$-NaCl. i=15 mA.
D: 5% PbS in $PbCl_2$-NaCl. i=50 mA.
R: Theoretical rate at 100% current efficiency.

shown in Fig. 5. The four curves measured at 530°C for different melt compositions and current densities show that a similar number of

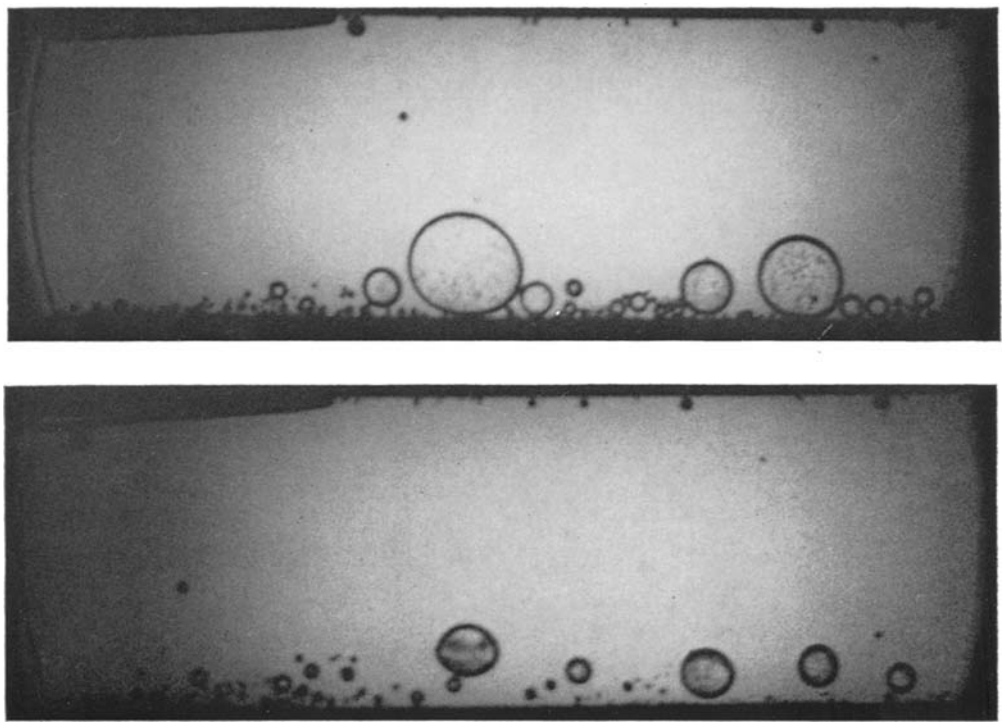

Fig. 3. (A) Sulphur gas bubbles forming during electrolysis. (B) Bubbles subsequently dissolving.

facing p. 26

coulombs are required in each case, before the steady rate of evolution is approached. The differences in the slopes between the calculated and steady state evolution rate is due to the dissolution of the gas. This in turn prevents the measurement of a net R.G.E. after electrolysis ceases.

by an inflexion in the bubble volume–time curve and a maximum in the dissolution rate. The dissolution rate is calculated from the change in bubble volume and surface area of contact. This is readily seen for the C curves of both Figs. 6 and 7. Fairly accurate compensation for this effect can be made by extrapolating that section

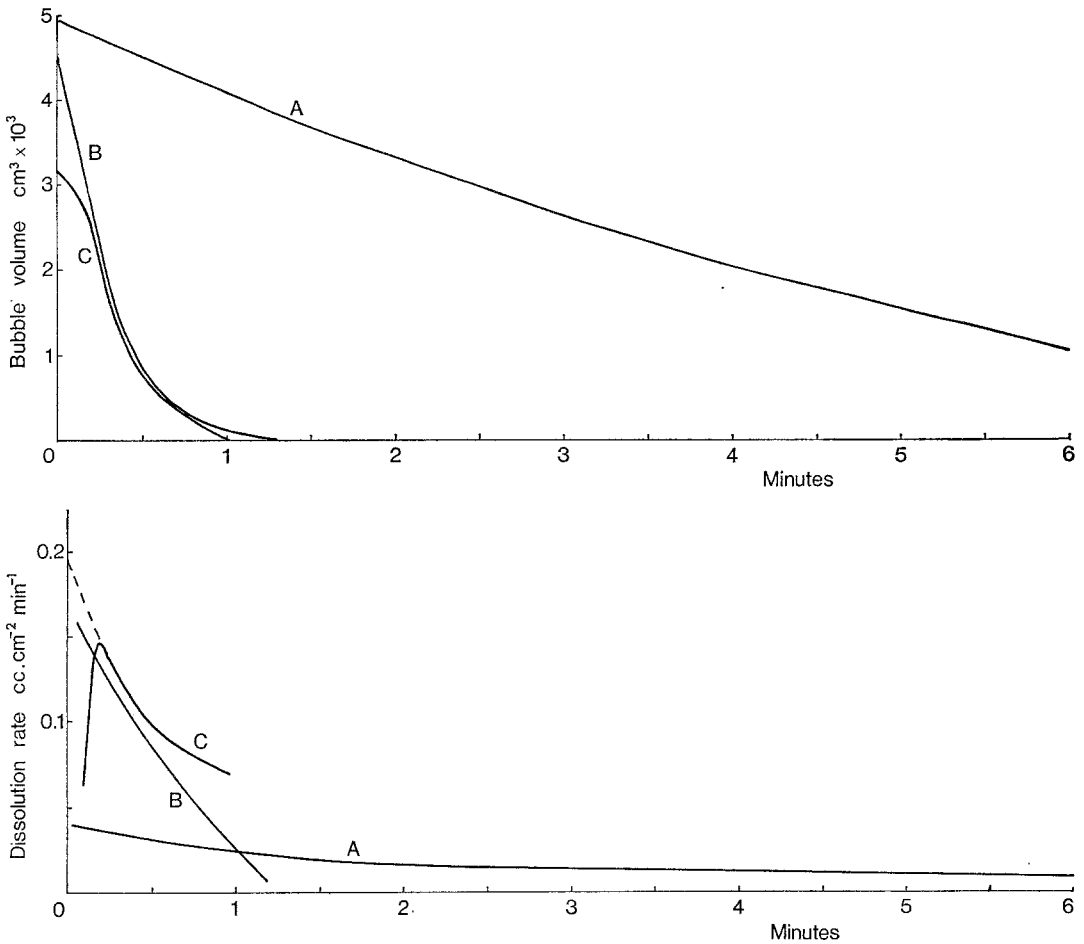

Fig. 6. Bubble volume and dissolution rate as a function of time for different temperatures and electrolytes. A: 5% PbS in $PbCl_2$-NaCl at 445°C. B: 5% PbS in $PbCl_2$-NaCl at 530°C. C: 20% PbS in $PbCl_2$ at 530°C.

3.2 *The rate of dissolution of gas*

On cessation of electrolysis the dissolution of the gas that was produced can be observed. The interpretation of the data in terms of rate of dissolution is complicated and will be treated in greater detail elsewhere [14].

Firstly, the results are complicated by R.G.E. whilst the bubble remains in contact with the electrode surface. Such an effect is characterized of curve not influenced by R.G.E. in a manner also illustrated in the figures.

A second complication can be seen from a consideration of the rate equation. The dissolution process may be expected to involve either gas–liquid absorption or alternatively involve chemical reaction. In either case it will be diffusion controlled across the interface area, since the thin cell cross-section and isothermal conditions will prevent convective mass transfer.

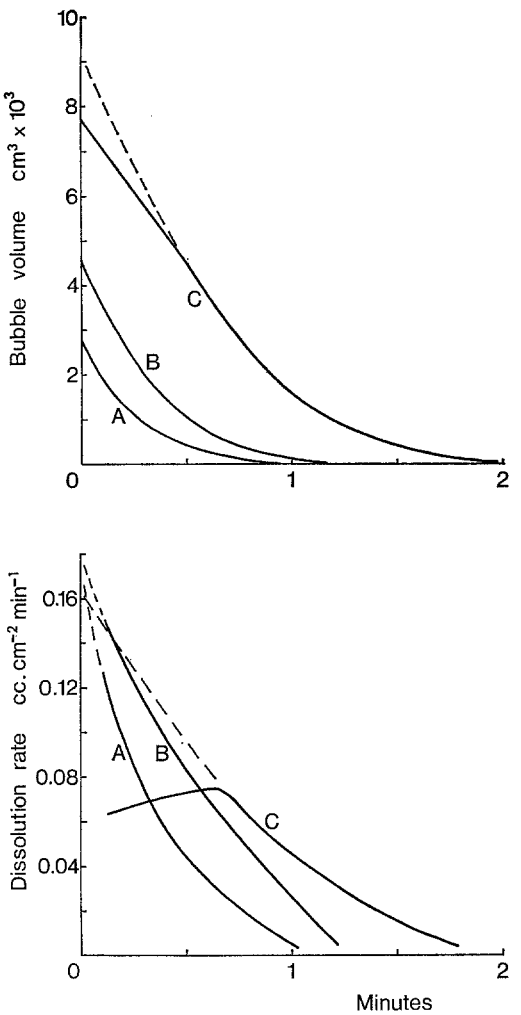

Fig. 7. Effect of bubble size on the rate of dissolution of sulphur. Electrolyte—5% PbS in $PbCl_2$-NaCl at 530°C.

In this case, however, the diffusion path is being continuously changed due to the shrinking of the gas bubble. Thus if we assume, for example, that the process involves a reaction and obeys first order kinetics, the appropriate equation for the rate of absorption per unit area of surface ($\Psi(t)$) at a stagnant surface [15] which is

$$\Psi(t) = c^* \sqrt{Dk}\ (\text{erf}\ \sqrt{kt} + (\exp(-kt))/\sqrt{\pi kt})$$

(where c^* is the saturated concentration of the solute (gas) at the interface, D the diffusion coefficient, k the rate constant, and t the reaction time) must be modified to allow for the shrinkage effect. This modification is dependent on both initial bubble size and reaction time.

Nevertheless, a good comparison between reaction rates under various conditions can be made if the initial bubble sizes are similar. A comparison of this type is made in Fig. 6 for both bubble volume and reaction rate as functions of time. The time of dissolution at 445°C (curve A) was over an order of magnitude greater than at 530°C and consequently the full curve measured is not illustrated. The results show that the rate of dissolution increases with increase in both temperature and sulphide concentration.

From bubbles of different size the initial rate of dissolution should be the same if there are no R.G.E. effects. This is because there would have been little disruption of the diffusion layer from the bubble shrinking, as reaction time tends to zero. Fig. 7 illustrates this point although only moderate agreement is found when bubble sizes differ by an order of magnitude. However, the agreement illustrated in Fig. 7 shows the value of the method especially when it is desirable to evaluate the dependent parameters of the rate equation.

4. Discussion and Conclusions

The examples used have served to illustrate the value of the optical cell described as a supplementary tool for electrode kinetic interpretations.

As a result of the optical studies we have established that the formation of sulphur from dissolved lead sulphide involves the formation of a chemisorbed species as a reaction intermediate. The method can detect this even when R.G.E. cannot be measured because of the dissolution process involving sulphur.

Illustration has also been made of the value of the method in determining whether an electrochemically generated gas undergoes dissolution. When this does occur it enables measurement of the rate of dissolution, and if successive electrolyses are carried out on the sample an estimate of the solubility of the gas is also possible. These findings in turn are useful in understanding losses in current efficiency during fused salt electrowinning processes.

Although the method described involved the use of borosilicate glass, and consequently introduced limitations on both temperature and electrolytes, we see no reason why the method

cannot be extended. The working temperature can be raised by the use of fused silica or Vycor, and if these materials introduce contamination problems polished single crystal alumina offers another alternative.

Acknowledgements

The authors would like to express their appreciation of assistance given by David M. Stitt and George Pashuk in the loan of lens systems and 16 mm filming system, respectively.

References

[1] A. K. N. Reddy, M. A. Genshaw and J. O'M. Bockris, *J. Electroanal. Chem.*, **8** (1964) 406.
[2] W. W. Hansen, T. Kuwana and R. A. Osteryoung, *Anal. Chem.*, **38** (1966) 1810.
[10] L. J. J. Janssen and J. G. Hoogland, *Electrochimica Acta*, **15** (1970) 941.
[11] C. N. Reilley, *Rev. Pure and Applied Chem.*, **18** (1968) 137.
[12] H. Braune, S. Peter and V. Neveling, *Z. Naturforsch.*, **6a** (1951) 32.
[13] P. L. King, Ph.D. Thesis, Univ. of New South Wales (1971).
[14] B. J. Welch and P. L. King, to be published.
[15] P. V. Danckwerts, *Trans. Faraday Soc.*, **46** (1950) 300.
[3] D. Landolt, R. Acosta, R. H. Muller and C. W. Tobias, *J. Electrochem Soc.*, **117** (1970) 839.
[4] L. J. J. Janssen and J. C. Hoogland, *Electrochimica Acta*, **15** (1970) 1667.
[5] J. Thonstad and A. Solbu, *Trans. Met. Soc. AIME*, **242** (1968) 301.
[6] D. A. J. Swinkels, *J. Electrochem. Soc.*, **113** (1966) 6.
[7] P. L. King and B. J. Welch, to be published.
[8] J. Thonstad, *J. Electrochem. Soc.*, **111** (1964) 955.
[9] S. Gjerstad and B. J. Welch, *J. Electrochem. Soc.*, **111** (1964) 976.